I&EC research
Industrial & Engineering Chemistry Research

Article

pubs.acs.org/IECR

Inverse Problems in Population Balances. Determination of Aggregation Kernel by Weighted Residuals

Jayanta Chakraborty,[†] Jitendra Kumar,[‡] Mehakpreet Singh,[‡] Alan Mahoney,[¶] and Doraiswami Ramkrishna*,[¶]

[†]Department of Chemical Engineering, and [‡]Department of Mathematics, Indian Institute of Technology Kharagpur, Kharagpur, 721302, India

[¶]Purdue University, West Lafayette, Indiana 47907, United States

Supporting Information

ABSTRACT: The phenomenology of particulate systems are embedded into the population balance model through breakage, aggregation, or growth kernels. Aggregation kernel is a difficult kernel to predict from first principle because of its nonlinear nature. In this work we demonstrate a new methodology to obtain the aggregation kernel through inverse problem approach. This new approach is based on the method of weighted residuals and does not rely on specific traits of the system like self-similarity. The residual approach reduces the inverse problem into solution of a set of linear equations. However, the system of equations is badly conditioned and therefore requires regularization for accurate solution. In this work Tikhonov regularization technique has been used. The new method has been demonstrated successfully for constant, sum, and product kernel.

INTRODUCTION

In the hope of providing a reasonable explanation for contributing to a special issue for one's own felicitation, this paper is an attempt to bring to the forefront the subject of inverse problems that we believe to be an essential aspect of identifying population balance models. While there have been a few publications in the past demonstrating the importance of inverse problems, the overwhelming approach to the use of population balances has been through force-fitting parameters in models that are either empirical or based on mechanisms of uncertain validity. Satisfactory fits often lend unwarranted support to the model as they are frequently under restricted conditions. The paper by Mahoney et al.[1] demonstrates the risks of such fitting. Yet, we wish not to be disparaging of the ever increasing effort on the use of population balance models, as their presence in engineering analysis, design, and control is a reflection of their high relevance to many dispersed phase processes encountered in engineering technology. Because of the ill-posed nature of inverse problems, without appropriate numerical armory to counter its effect, their solution is often difficult. It is our objective in this paper to show some success in this regard and possible directions for the future. Specifically, this work introduces a new technique for extraction of aggregation kinetics using the inverse problem approach.

Modeling of aggregation is one of the major areas[2,3] in population balances. Aggregation is the process whereby two or more particles come together and remain bound for long enough to be considered a unique new particle. Two subprocesses are considered important: First, the frequency at which particles come near enough to one another so that they can interact with each other. This is generally termed the collision frequency, and is a well explored area. Smoluchowski[4] predicted the collision frequencies for particles moving by Brownian motion and in laminar shear fields. In another major study, Drake[5] investigated collisions in turbulent fields (collisions due to inertial effects and diffusion).

Once the particles have come into contact, a second subprocess can be modeled to predict the efficiency of the collision, whether the particles remain together. For droplets, this has been predicted using film-drainage models by Muralidhar and Ramkrishna.[6] For granulation processes, Ennis et al.[7] developed a model which measures the ratio of granule collisional kinetics energy to the viscous dissipation to model the efficiency. For crystallization or precipitation particles, Hounslow et al.[8] and Hounslow et al.[9] have developed a model based on the ratio of the strength of necks formed by deposited material to the straining force of the surrounding fluid. The experimental system was a differential reactor, allowing the rapid study of aggregation under many different conditions.

The current modeling of particulate processes involves diverse approaches including direct observation of particles or populations followed by model parameter estimation or inverse problem techniques to quantify the models. The distinction arises between the *a priori* assumptions of model form as required for direct parameter estimation and the more general form allowed in inverse problem formulation. The advantage of a more flexible form is balanced by the requirement for more free parameters and therefore more experimental data. However, this becomes an attractive approach when suitable models have been tried and found to be elusive.

Special Issue: Doraiswami Ramkrishna Festschrift

Received: April 14, 2015
Revised: June 17, 2015
Accepted: June 22, 2015
Published: June 22, 2015

DOI: 10.1021/acs.iecr.5b01368
Ind. Eng. Chem. Res. 2015, 54, 10530−10538

The most direct method of evaluating particle kinetics is the observation of individual particles to determine their behavior. This is difficult for aggregating systems where particles must be followed and their interactions must be monitored to observe collision effects. A tracking technique has been applied for studying the growth, but not for the aggregation of crystals.[10]

Inverse problems arise mathematically when the solution to a differential or integro-differential equation is known, but phenomological functions in the model are not. While solutions to these problems can be derived in a number of cases, these problems are often ill-conditioned, and noise as well as discretization of experimental measurements obviates approximate numerical methods. Inverse problem methods are particularly attractive in the absence of *a priori* knowledge of appropriate forms for particle dynamic laws, since the form can be determined directly from the experimental data. Besides, they can also serve to assess the veracity of candidate physical models since the result can be compared with the model forms.

Inverse problem solution techniques for population dynamics have been long pursued by Ramkrishna,[11] including the use of self-similarity to determine aggregation[12] and breakage[13−16] laws. The technique is similar to that used by Thompson[17] in developing his empirical aggregation kernel for aerosol coalescence. These techniques rely, however, on specific traits of the system, for example, self-similarity, that depend on both the aggregation kernel and initial condition. In the presence of significant particle growth, self-similarity is not achieved, requiring other techniques. Mahoney et al.[1] have shown the inverse problem technique where the growth and aggregation may be decoupled and obtained. Bramley et al.[18,19] have applied a combination of inverse-problem and parameter estimation techniques, using the dynamic variation of the zeroth and third moments of the distribution to calculate time-varying growth, aggregation, and nucleation parameters.

Recent studies on inverse problem are more centered around breakage problems. Self-similarity has been a key assumption in the majority of such works[13−16,20−23] involving the inversion of breakage equation. Kostoglou and Karabelas[24] presented a work focused on the sensitivity of the relationship between self-similar particle size distributions and breakage kernel. Kostoglou and Karabelas[25] found the deterministic breakage rate using the framework of statistical theory and demonstrated the method to derive existing models (deterministic laws) in a systematic and consistent way. Maaß and Kraume[26] have presented a technique to solve the breakage population balance equation for the determination of breakage laws using single drop experiments.

The current work introduces a simple technique based on weighted residuals for performing the inverse problem for generation of the aggregation law. This is especially applicable in areas where the full kinetics resulting from multiple effects (turbulence, collision frequency, and efficiency) are not yet understood. The method of weighted residuals (MWR) converts the inverse problem to an ill-posed system of linear equations. Therefore, the issue of ill-posedness is addressed and some directions for stabilizing the solution are given. In particular, a detailed analysis of the impact of data smoothness and scaling on solution properties is performed using some examples.

METHOD OF WEIGHTED RESIDUALS

The population balance equation (PBE) expresses the relationship between the kinetics of individual particles and the dynamics of the entire population distribution. The population balance equation used here is based on a continuous particle size distribution. This can be derived either from a direct balance on the number density, or as the expectation of the underlying true discrete number density.[11]

There are two common choices for the particle size dimension, particle length, or volume. While mathematically equivalent, there are practical numerical considerations for the formulation. If length is chosen as an internal coordinate, the Jacobian term in the aggregation birth term is non-unity while for volume it is unity. For the formulation of method of weighted residual, we consider the one-dimensional pure aggregation population balance equation in volume coordinates as

$$\frac{\partial f(v,\,t)}{\partial t} = \frac{1}{2}\int_0^v \beta(v-u,\,u,\,t)\, f(v-u,\,t)\, f(u,\,t)\,\mathrm{d}u - \int_0^\infty \beta(v,\,u,\,t)\, f(v,\,t)\, f(u,\,t)\,\mathrm{d}u \tag{1}$$

Here $t \geq 0$ and $f(v,t)$ is the transient number density distribution. The first term represents the birth of the particles of size v as a result of the coagulation of particles of sizes $(v-u)$ and u. Here we shall refer to size as the particle volume. The second term describes the merging of particles of size v with particles of other sizes. The second term is called the death term. The nature of the process is governed by the coagulation kernel β representing properties of the physical medium. It is non-negative and satisfies the symmetry condition $\beta(u,\,v,\,t) = \beta(v,\,u,\,t)$. The insertion of time in the aggregation kernel is because of the uncertainty involved in the existence of a time-independent kernel to describe the aggregation process.

Residual Formulation. The method of weighted residuals[27] can be used for forward simulation of population balance equations. We wish to approximate the number density function f by a function $\tilde{f}$, which is a linear combination of basis (shape) functions φ_j chosen from a linearly independent set. That is,

$$f(v,\,t) \cong \tilde{f}\,(v,\,t) = \sum_{j=1}^{n} \alpha_j(t)\varphi_j(v) \tag{2}$$

Note that the coefficients are made a function of time to incorporate the variation of number density with time. It is also important that the approximate solution satisfies the required boundary conditions. Upon substitution of this form into the PBE (1) and arranging all the terms in the left to yield a nonzero residual the equation becomes

$$\mathfrak{R} = \left(\frac{\partial \tilde{f}\,(v,\,t)}{\partial t} - \frac{1}{2}\int_0^v \beta(v-u,\,u,\,t)\,\tilde{f}\,(v-u,\,t)\,\tilde{f}\,(u,\,t)\,\mathrm{d}u + \int_0^\infty \beta(v,\,u,\,t)\,\tilde{f}\,(v,\,t)\,\tilde{f}\,(u,\,t)\,\mathrm{d}u\right) \tag{3}$$

The notion in the MWR is to force the residual to zero in some average sense over the domain. In other words, the unknown coefficients α_j are obtained at any time in such a way that the inner product of the residual with a suitably chosen weighting function becomes identically zero. Mathematically:

$$\int_0^\infty \mathfrak{R}\,\psi_i(v)\,\mathrm{d}v = 0, \qquad i = 1,\,2,\,\ldots n \tag{4}$$

DOI: 10.1021/acs.iecr.5b01368
Ind. Eng. Chem. Res. 2015, 54, 10530−10538

where the number of weight functions ψ_i is exactly equal the number of unknown coefficients α_j in $\tilde{f}$. This results in a system of ordinary differential equations for the unknown coefficients α_j. Once the coefficients α_i are known, they can be used in (2) to approximate the number density f. Note that the accuracy of the solution $\tilde{f}$ depends on the choice of basis functions.

We adapt this approach for identifying the aggregation kernel in the following way: first, the aggregation kernel is written approximately in terms of a finite set of basis functions and unknown coefficients:

$$\beta(u, v, t) \cong \tilde{\beta}(u, v, t) = \sum_{j=1}^{n} \alpha_j(t)\, \phi_j(u, v) \tag{5}$$

whose substitution into the aggregation PBE generates the residual:

$$\Re = \frac{\partial f(v, t)}{\partial t} - \sum_{j=1}^{n} \alpha_j \frac{1}{2} \int_0^v \phi_j(v - u, u, t)\, f(v - u, t)\, f(u, t)\, \mathrm{d}u - \int_0^\infty \phi_j(v, u, t)\, f(v, t)\, f(u, t)\, \mathrm{d}u \tag{6}$$

Note that the equation for the residual, while nonlinear (quadratic) in the measured (known) number density, f, is linear in the coefficients of expansion for the aggregation kernel. This greatly simplifies the numerical analysis. Now proceeding as before with an additional integration over time between $[t_k, t_{k+1}]$, we obtain

$$\int_{t_k}^{t_{k+1}} \mathrm{d}t \int_0^\infty \Re\, \psi_i(v)\, \mathrm{d}v = 0, \qquad i = 1, 2 \ldots n \tag{7}$$

The aggregtion kernel (and hence the unknown coefficients) may be considered to be constant over a reasonably short time scale, that is, between $[t_k, t_{k+1}]$. This leads to the following system of linear equations in unknown α_i's,

$$\mathbf{A}\alpha = \mathbf{b} \tag{8}$$

where the coefficients of the matrix $\mathbf{A}$, for each k, are given by

$$A_{i,j} = \frac{1}{2} \int_{t_k}^{t_{k+1}} \mathrm{d}t \int_0^\infty \psi_i(v)\, \mathrm{d}v \int_0^v \phi_j(v - u, u, t)\, f(v - u, t)\, f(u, t)\, \mathrm{d}u - \int_{t_k}^{t_{k+1}} \mathrm{d}t \int_0^\infty \psi_i(v)\, \mathrm{d}v \int_0^\infty \phi_j(v, u, t)\, f(v, t)\, f(u, t)\, \mathrm{d}u \tag{9}$$

The ith component of the right-hand side vector $\mathbf{b}$, is given as

$$b_i = \int_0^\infty \psi_i(v)[f(v, t_{k+1}) - f(v, t_k)]\, \mathrm{d}v \tag{10}$$

The above system of equations needs to be solved for each pair of measurements $[t_k, t_{k+1}]$to advance the system in times.

The next step is to choose an appropriate shape function. Polynomials are usually chosen as shape functions. In this work we have taken the bilinear shape functions over square elements. A typical square element is shown in Figure 1 along with the notation. The shape function at the node i of an element e has value 1 at the node i and vanishes over any element boundary that does not include the node i. Thus, for a given element we have at the node

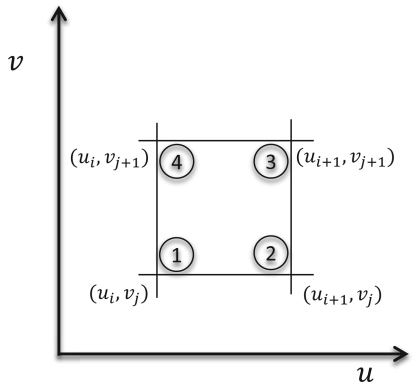

Figure 1. Generation of bilinear basis functions.

$$①: \quad \phi_1^e(u, v) = \frac{(u - u_{i+1})(v - v_{j+1})}{(u_i - u_{i+1})(v_j - v_{j+1})}$$

$$②: \quad \phi_2^e(u, v) = \frac{(u - u_i)(v - v_{j+1})}{(u_{i+1} - u_i)(v_j - v_{j+1})}$$

$$③: \quad \phi_3^e(u, v) = \frac{(u - u_i)(v - v_j)}{(u_{i+1} - u_i)(v_{j+1} - v_j)}$$

$$④: \quad \phi_4^e(u, v) = \frac{(u - u_{i+1})(v - v_j)}{(u_i - u_{i+1})(v_{j+1} - v_j)}$$

Typical bilinear shape functions at the intersection of four square elements are shown in Figure 2. It may be noted that the value of the ith coefficient is same as that of the kernel at the ith node.

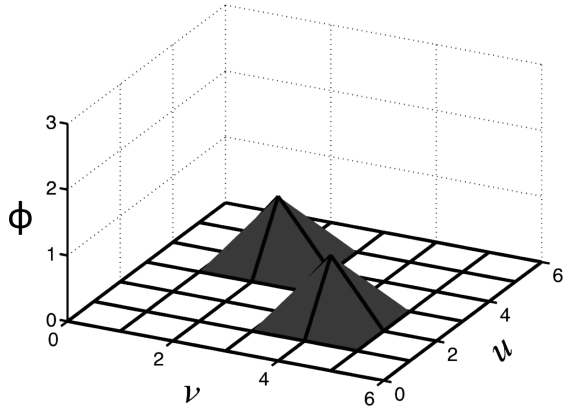

Figure 2. Typical local bilinear basis functions used in this study.

Once the shape functions are decided, we must choose the weighting functions. The simplest weighting functions to use would be Dirac delta functions in size. In that case, the method becomes that of collocation. However, the method is not limited to this simplest weighting function as any other weighting functions may also be used if required. A constant weighting function $\psi(v) = 1$ may also be used but it will produce only one equation for each measurement of system. This has been used by Bramley et al.[18] to determine a single constant for a priori known size dependency of aggregation law. In this work, Dirac delta functions in size, that is, $\psi_i(v) = \delta(v - v_i)$, are chosen for easy evaluation of the particle size integral.

DOI: 10.1021/acs.iecr.5b01368
Ind. Eng. Chem. Res. 2015, 54, 10530−10538

In this case, the coefficient matrix **A** and the right-hand side vector **b** become

$$A_{i,j} = \frac{1}{2}\int_{t_k}^{t_{k+1}} \mathrm{d}t \int_0^{v_i} \phi_j(v_i - u, u, t) f(v_i - u, t) f(u, t)\, \mathrm{d}u - \int_{t_k}^{t_{k+1}} \mathrm{d}t \int_0^{\infty} \phi_j(v_i, u, t) f(v_i, t) f(u, t)\, \mathrm{d}u \quad (11)$$

and

$$b_i = [f(v_i, t_{k+1}) - f(v_i, t_k)] \quad (12)$$

This completes the formulation of the method of weighted residuals.

RESULTS AND DISCUSSION

In this section, we focus on extraction of approximate aggregation laws using the proposed method. We test for three most popular empirical kernels, namely, constant, sum, and product kernel.

Extraction of the Constant Kernel. Various parameters for the forward problem for the constant kernel case is summarized in Table 1. First, the forward problem has been solved and data is generated on 100 linearly spaced grid points in size and 10 linearly spaced points in time as shown in Figure 3a. It can be seen that the number density is well contained in the region chosen and forms a well behaved monotonic surface. The aggregation kernel has been described in terms of nine basis functions in v–v' space. For the Dirac-delta functions (weights), six linearly spaced points in particle size between 0 and 13 have been chosen because six equations are needed. The remainder of the equations will be obtained by using symmetry. Time limits are taken from 0 to 1. In the following test problems we shall consider the kernels to be time independent and hence the coefficients will also be time independent.

Table 1. Parameters Used for Forward Problem: Constant Kernel Case

parameter	value
$\beta(v, v')$	1
$f(v, 0)$	$\exp(-v)$
$f(v, t)$	$(4/(t+2)^2)\exp(-2v/(t+2))$

The basis functions (ϕ) have been defined as bilinear functions on the two-dimensional coarse grid defined by $v = v' = [0, 6.5, 13]$, for a total of 9 basis functions as shown in Figure 4. All integrations are performed using the recursive adaptive Simpson quadrature method using the function `dblquad` in MATLAB. This finally leads to a system of nine linear equations in nine unknown α_i's,

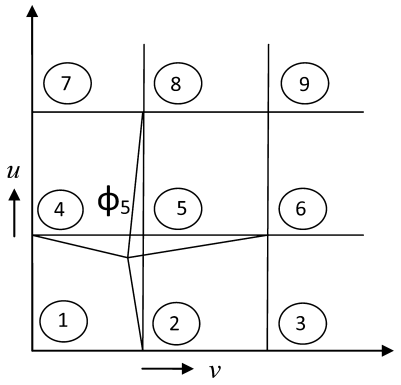

Figure 4. Elements and nomenclature of nodes for a discretized domain.

$$\mathbf{A}\alpha = \mathbf{b} \quad (13)$$

where **A** is given as shown in Chart 1 and the right-hand side vector obtained from eq 12 is given by

$$\mathbf{b} = [\,-0.0098\ \ 0.0116\ \ 0.0043\ \ 0.0012\ \ 0.00031\ \ 7.428 \times 10^{-5}\ \ 0\ \ 0\ \ 0\,]^{\mathrm{T}}$$

It may be noted that the last three equations have been obtained using symmetry. It is evident from the nature of **A** that the system of equations is badly conditioned. The condition number of the matrix **A** is 1.57×10^9 and hence, the inversion may not be accurate. The result of the inversion has been shown in column 2 of Table 2. where this set of equations is solved for α's using Matlab command `linsolve`. It may be seen that for most of the nodes the inversion is successful but significant deviation occurs to the nodes where the population is very less. One of the ways to circumvent this problem is to use regularization techniques. In this work we use Tikhonov regularization to improve the accuracy of the solution. The details of the method including the regularization parameter used has been provided in the Supporting Information. Column 3 of the same table shows the result using the Tikhonov regularization. As expected, the results show improvement for

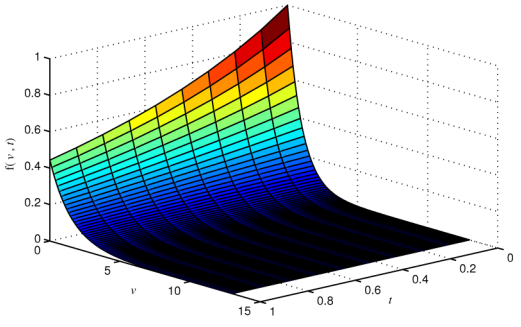

(a) Without noise

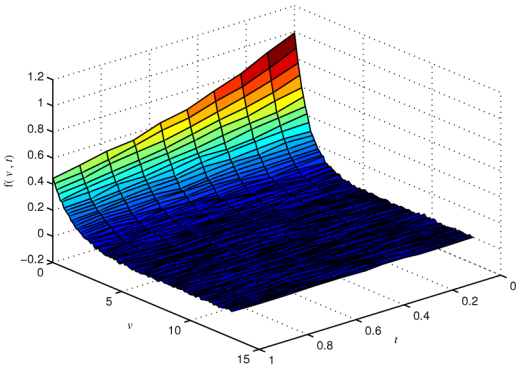

(b) With 4% white Gaussian noise.

Figure 3. Evolution of number density for constant kernel.

DOI: 10.1021/acs.iecr.5b01368
Ind. Eng. Chem. Res. 2015, 54, 10530−10538

Chart 1

$$\begin{bmatrix}
6.45\times10^{-3} & -0.0126 & 0 & 7.14\times10^{-3} & -4.17\times10^{-3} & 0 & -6.63\times10^{-5} & 3.31\times10^{-5} & 0\\
6.89\times10^{-3} & -1.33\times10^{-3} & 0 & 6.07\times10^{-3} & 3.13\times10^{-5} & 0 & -6.42\times10^{-6} & -1.28\times10^{-5} & 0\\
1.18\times10^{-3} & 1.33\times10^{-4} & 0 & 2.37\times10^{-3} & 6.43\times10^{-5} & 0 & 0 & -3.83\times10^{-6} & 0\\
6.36\times10^{-5} & 2.43\times10^{-4} & -7.37\times10^{-5} & 5.18\times10^{-4} & 4.09\times10^{-4} & -2.61\times10^{-5} & 6.38\times10^{-5} & 7.46\times10^{-6} & -2.59\times10^{-7}\\
1.49\times10^{-6} & 5.16\times10^{-5} & -1.05\times10^{-5} & 7.79\times10^{-5} & 1.32\times10^{-4} & -1.32\times10^{-6} & 4.20\times10^{-5} & 1.19\times10^{-5} & -1.07\times10^{-7}\\
0 & 7.84\times10^{-6} & 2.34\times10^{-7} & 7.84\times10^{-6} & 3.13\times10^{-5} & 3.85\times10^{-6} & 1.57\times10^{-5} & 7.84\times10^{-6} & -3.39\times10^{-8}\\
0 & 1 & 0 & -1 & 0 & 0 & 0 & 0 & 0\\
0 & 0 & 1 & 0 & 0 & 0 & -1 & 0 & 0\\
0 & 0 & 0 & 0 & 0 & 1 & 0 & -1 & 0
\end{bmatrix}$$

Table 2. Determined Coefficients for the Constant Kernel Problem[a]

	9 × 9	9 × 9	8 × 8	8 × 8	8 × 8	9 × 9
α	wo Reg.	w Reg.	wo Reg.	w Reg.	wo Int. w Reg.	4% wGn
α_1	0.9863	0.9863	0.9899	0.9899	1.0001	0.833
α_2	1.0018	1.0120	1.0097	1.0097	1.0003	1.3
α_3	1.0776	1.0130	1.0297	1.0314	0.9978	0
α_4	1.0118	1.0120	1.0097	1.0097	0.9998	1.3
α_5	0.9760	0.9754	0.9806	0.9805	1.0001	0
α_6	0.9280	1.0075	0.9886	0.9646	1.0188	0
α_7	1.0776	1.0310	1.0298	1.0314	1.0023	26.86
α_8	0.9280	1.0075	0.9686	0.9646	0.9810	0
α_9	5.2092	0.2959	0.9806	0.9805		0
cond(**A**)	1.57×10^9	1.57×10^9	3.47×10^5	3.47×10^5	3.48×10^5	8.1×10^9

[a]True values for $\alpha_1 \cdots \alpha_9 = 1$. Annotation: wo, without; w, with. wo Reg, without using Tikhonov regularization; wo Int.; using the analytical function value at all necessary intermediate points for integration instead of using interpolation. This removes the interpolation error. 4% wGn: Results obtained by adding 4% white Gaussian noise to the number density data.

node points which have low population density (nodes 3, 6, 7, 8, and 9). However, the last node (node 9) could not be predicted accurately.

The inversion requires product of number density at v and v' which is very small at the upper right corner point of the $v - v'$ domain. Hence, it is unlikely that an aggregation kernel be found accurately at this point. We need to have an alternate strategy for finding the kernel at such sparse nodes. We have used extrapolation using the Matlab function `gridfit` successfully to obtain the aggregation kernel for the ninth node. Since the ninth point can be obtained using extrapolation, the last rows and columns of the coefficient matrix may be omitted altogether, and one can solve the resulting 8 × 8 system instead. This improves the condition number of the matrix over 3 orders of magnitude. The results of the inversion has been shown in Table 2, column 4. Interestingly, this does not improve the solution significantly, and rather the eighth node was predicted poorly.

It may be noted that the major reason for the large condition number of the matrix is the area containing a very small population. One may tend to think that restricting the domain to only a large population may remove this problem. However, our simulations show the opposite: if we remove the tail, the integrations become inaccurate which leads to grossly inaccurate results. Also making a finer grid not necessarily improves the inversion. It leads to more number of elements with even smaller values and a few with larger values. The condition number swells to a very large value and inversion becomes more difficult. For example, if we use a 16 node grid instead of 9 node grid, the condition number of the matrix **A** jumps to 10^{11} which leads to inaccurate values of the coefficients.

It appears from the foregoing discussion that accurate evaluation of the integral is important. To check whether the accuracy of the integral is affected by the accuracy of the interpolation, we run the inversion with exact solution of the forward problem instead of using interpolation of the synthetic data. The result has been shown in column 6 of Table 2. It can be seen that results improve slightly which signify that the interpolations were accurate. It also implies that monitoring the accuracy of the interpolation is important. However, much stress cannot be given toward this end because data may have significant noise.

To test whether noise in the data can be dealt with using this method, we added 4% white Gaussian noise to the exact solution (see Figure 3b). The result of inversion using the noisy data are shown in Table 2, column 7. It can be seen that the noise gives inaccurate results at low population nodes, but results are reasonably accurate where population density is high.

Extraction of Sum Kernel. Now, we apply the inverse problem methodology to a more difficult situation. The number density function for sum kernel has been shown in Figure 5. It can be seen that the function chosen is nonmonotonous (as given in Table 3) and shows a sharp maxima near the small volume limit. The number density also falls very rapidly with volume after this maximum. However, the domain must be extended to a larger value to avoid significant domain loss. This makes this problem more challenging than the constant kernel case. The data has been generated at linearly spaced points in particle volume between 0 and 80 and the time domain is divided into 10 linearly spaced points from 0 and 1.3. The aggregation kernel has been described in terms of nine basis functions as before in a two-dimensional coarse grid defined by $v = v' = [0, 40, 80]$. Dirac points are also chosen in the same manner.

The major feature for inversion for this case is that the data should be available in a finer mesh, at least in the region of sharp variation in number density. Otherwise, the interpolation error will be significant. The inversion results are shown in

DOI: 10.1021/acs.iecr.5b01368
Ind. Eng. Chem. Res. 2015, 54, 10530−10538

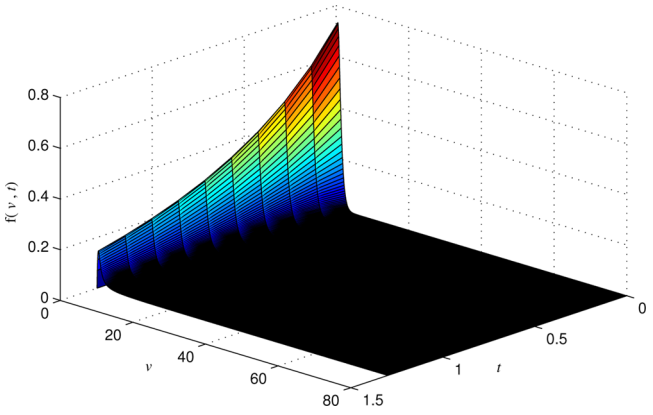

Figure 5. Evolution of number density for sum kernel. The sharp peak near the small volume limit may be noted.

Table 3. Parameters Used for Forward Problem: Sum Kernel Case[29]

$\beta(v, v') = v + v'$
$N_0 = 1,\ v_0 = 1$
$f(v, 0) = \exp(-v)$
$\tau = 1 - \exp(-T_a)$
$f(v, t) = (N_0/v_0)\phi(x,T_a)$ where $x = v/v_0$ and $T_a = N_0 v_0 t$
$\phi(x,T_a) = (1 - \tau)\exp[-(\tau + 1)x]\sum_{k=0}^{\infty}((\tau^k x^{2k})/((k + 1)!\ \Gamma[(k + 1)]))$

Table 4. It can be seen that the coefficients are predicted with reasonable accuracy except the last node. Tikhonov regularization helped to improve the accuracy of most of the nodes, but the accuracy of a few nodes have been mildly affected by the regularization. Solving a reduced system (8×8) did not improve the condition number dramatically, and solutions are of a similar nature as those obtained by a full (9×9) system. In this case also we check the accuracy of interpolation, and the results using the analytical solution are shown in last column of Table 4. It may be seen that the results improved slightly signifying that interpolations were reasonably accurate. The last column of Table 4 shows the case where data with 4% white Gaussian noise is used. Like a previous case, the low population nodes are not predicted well, but the high population nodes are predicted with reasonable accuracy.

Extraction of Product Kernel. In this section, we extract the product kernel for which the parameters are given in Table 5. The solution of the forward problem for this case has been

Table 5. Parameters Used for Forward Problem: Product Kernel Case[29]

$\beta(v, v') = vv'$
$N_0 = 1,\ v_0 = 1$
$f(v, 0) = \exp(-v)$
$f(v, t) = (N_0/v_0)\phi(x,\tau)$ where $x = v/v_0$ and $\tau = N_0 v_0^2 t$
$\phi(x,\tau) = \exp[-(\tau + 1)x]\sum_{k=0}^{\infty}((\tau^k x^{3k})/((k + 1)!\ \Gamma[2(k + 1)]))$

shown in Figure 6. It can be seen that like constant kernel, the plot of the forward problem is a monotonic surface. However,

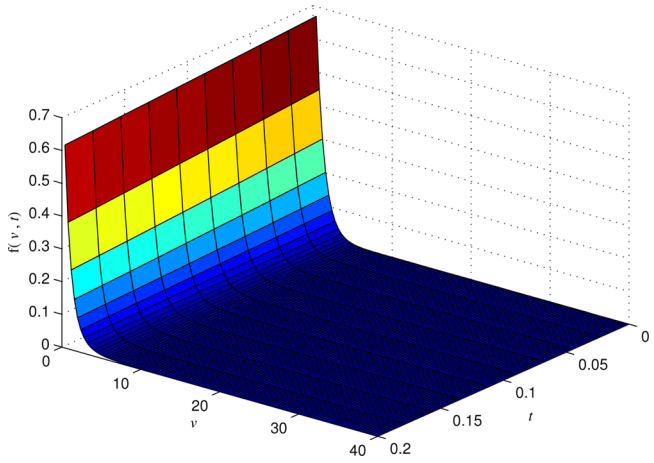

Figure 6. Evolution of number density for product kernel.

as we will see, the inverse problem rightly identifies the difference. Here the kernel is zero at the axes and hence the domain should be divided into smaller parts to obtain nonzero values of the aggregation kernel inside the domain. However, at the beginning we shall assume no such knowledge about the kernel and start with the same coarse elements. The values of different α's are shown in Table 6. It can be seen that the value of the kernel has been extracted within 1% on nodes which has nonzero value of the kernel, except the sparsest node. However, it produces nonzero values for the nodes where the true kernel value is zero. The value, however, is small compared to the kernel value at other places and the kernel may be considered to be reasonably extracted over the domain. Regularization using Tikhonov regularization has been tried for this problem

Table 4. Determined Coefficients for the Sum Kernel Problem[a]

		9×9	9×9	8×8	8×8	9×9
α	true values	w Int. wo Reg.	w Int. w Reg.	w Int. wo Reg.	wo Int. wo Reg.	4% wGn
α_1	0	−0.326	−0.145	−0.114	0.0117	0.1527
α_2	40	40.86	40.29	40.167	39.727	27.78
α_3	80	81.63	74.02	77.788	78.898	62.08
α_4	40	40.86	40.29	40.167	39.727	27.78
α_5	80	73.90	78.34	75.808	78.463	57.81
α_6	120	107.53	137.08	114.73	117.38	0
α_7	80	81.63	74.02	77.788	78.898	62.08
α_8	120	107.53	137.08	114.73	117.38	0
α_9	160	17.04	146.58			0
cond(**A**)		1.5×10^9	1.50×10^9	1.7×10^8	1.8×10^8	

[a]Annotation: wo, without; w, with. wo Reg, without using Tikhonov regularization; wo Int., using the analytical function value instead of interpolated values; 4% wGn, results obtained by adding 4% white Gaussian noise to the number density data.

DOI: 10.1021/acs.iecr.5b01368
Ind. Eng. Chem. Res. 2015, 54, 10530−10538

Table 6. Determined Coefficients for the Product Kernel Problem[a]

α	α_{True}	α_{Inv} wo Reg	α	α_{True}	α_{Inv} wo Reg	α_{Inv} 4% wGn `lsqnonneg`
α_1	0	−0.045	α_1	0	0.0005	0
α_2	0	0.216	α_2	0	−0.0046	0.0038
α_3	0	0.523	α_3	0	−0.1946	1.249
α_4	0	0.216	α_4	0	−9.6741	0
α_5	400	398.4	α_5	0	−0.0046	0
α_6	800	796.5	α_6	177.76	177.70	177.76
α_7	0	0.523	α_7	355.55	356.43	348.62
α_8	800	796.5	α_8	532.33	565.25	536.58
α_9	1600	1056.9	α_9	0	−0.1946	0
			α_{10}	355.55	356.43	356.04
			α_{11}	711.12	771.30	0
			α_{12}	1066.6	1702.3	0
			α_{13}	0	−9.6741	0
			α_{14}	533.32	565.25	581.34
			α_{15}	1066.6	1702.3	0
			α_{16}	1600.0	−12785	0
cond(**A**)		1.25×10^{12}			3.96×10^{13}	

[a]Annotation: wo, without; w, with. wo Reg, without using Tikhonov regularization; wo Int., using the analytical function value instead of interpolated values; 4% wGn, results obtained by adding 4% white Gaussian noise to the number density data.

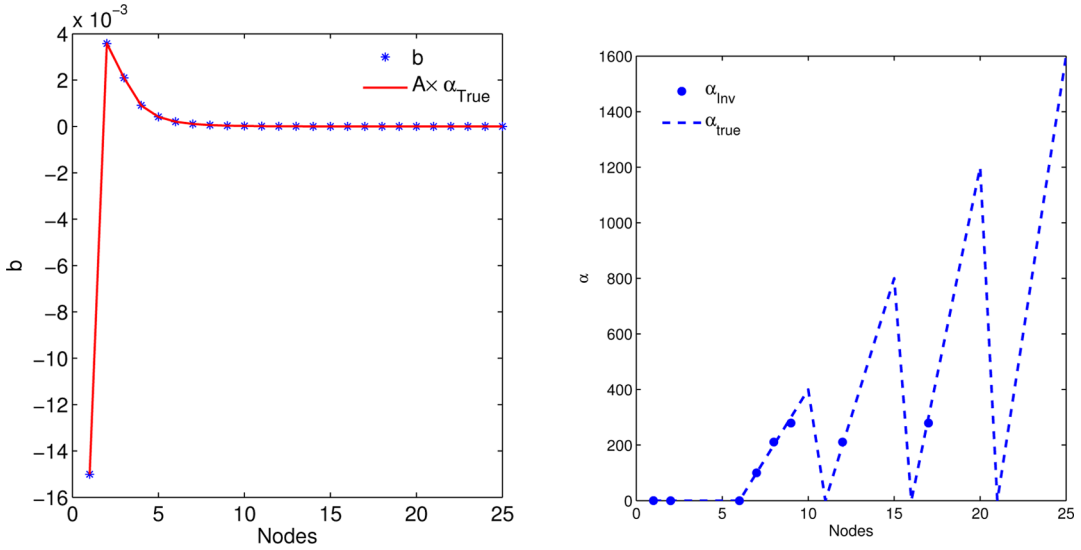

Figure 7. Inversion for the case of product kernel with 25 nodes. Although $\mathbf{A} \times \alpha$ matches exactly with **b**, the inversion is accurate only for 33% of nodes (Values differing more than an order have been omitted for clarity).

also but found to be ineffective for such a high-condition number.

The extraction with a finer mesh with 16 nodes has also been shown in Table 6. It can be seen that the condition number is one order more but the kernel has been extracted with reasonable accuracy. Like previous case, the zeros are predicted as small negative numbers. We tried with another solver `lsqnoneg` which is constrained to produce only a positive solution. Although it produces zeros in place of negative solutions, the accuracy of other nodes are reduced. The Tikhonov regularization also improves the solution only marginally. The last column shows the result where a small noise has been added to the data. The `linsolve` solver produced a lot of large negative values in this case (not shown). However, the constrained solver `lsqnoneg` worked very well for this case. The solutions are very accurate, and the method is successful even with noise. It seems that the solution of the ill conditioned set of linear equations is the vital step for inversion.

To investigate the case with even finer mesh, we increase the number of nodes to 25 and 100, respectively, and repeat the calculations. However, the condition number of **A** becomes very high for both the cases (10^{15} and 10^{28}, respectively). We attribute this to increase in the number of elements with an even higher difference in values. The result of the inversion with 25 nodes has been shown in Figure 7 (right). It can be seen that the quality of inversion is poor. To investigate whether the failure was due to any factor other than ill conditioning of the matrix, $\mathbf{A} \times \alpha_{true}$ has been compared with **b** as shown in Figure 7 (left). They show an exact match for both the 25-node and 100-node cases (result not shown). Hence, the failure of inversion in such fine meshes was due to ill conditioning of the linear system. If information over such finer mesh is required, a suitable regularization technique will be required. Using weight functions other than Dirac delta is also another option but that will require some minor changes in the formulation.

DOI: 10.1021/acs.iecr.5b01368
Ind. Eng. Chem. Res. 2015, 54, 10530−10538

CONCLUSIONS AND OUTLOOK

A new inverse problem methodology has been demonstrated in this work. This new strategy is based on the method of weighted residuals and has been demonstrated for the inversion of the aggregation population balance equation. This method does not depend on the existence of special traits for the system like self-similar behavior.

The new method has been demonstrated successfully for constant, sum, and product kernel. Like many inverse problems, this method also needs the solution of an ill-conditioned system of linear equations with condition number ranging from 10^9 to 10^{13}. The accuracy of inversion is therefore dependent on the effectiveness of the regularization technique. Tikhonov regularization has been used successfully in this work. However, a few issues should be considered for application of this method to noisy experimental data:

(1) Effect of noise: Simulations show that the accuracy of the inversion is dependent on the amount of noise present. The effect of noise is also dependent on the kernel. Some degree of noise cancellation is also possible because of the integral nature of the method. Casewise guidelines therefore may be obtained which will foretell the expected degree of accuracy if the signal-to-noise ratio of data is provided. It has also been observed that the tail of the PSD should be included for accurate inversion. But data over the tail region may contain larger noise than other regions of the PSD. For such a data set, the proper strategy for treating the tail data can be explored; for example, data smoothing may be used.

(2) Refinement of the grid: An important feature of this method is that the condition number of the linear system increases as the grid is refined. Hence, it is difficult to obtain more accurate results from a finer meshing in size domain. Scaling of the matrix, alternate weight function, and a more sophisticated regularization technique are possible remedies to this problem.

Improvement on these aspects should help evolve a robust tool toward inversion of experimental data on aggregation systems to obtain aggregation kernels.

ASSOCIATED CONTENT

Supporting Information

Tikhonov regularization as given by Press et al.[28] has been used. The details of the regularization parameter used is given. The Supporting Information is available free of charge on the ACS Publications website at DOI: 10.1021/acs.iecr.5b01368.

AUTHOR INFORMATION

Corresponding Author

*E-mail: ramkrish@ecn.purdue.edu.

Notes

The authors declare no competing financial interest.

REFERENCES

(1) Mahoney, A.; Doyle, F., III; Ramkrishna, D. Inverse problems in population balances: Growth and nucleation from dynamic data. *AIChE J.* **2002**, *48*, 981−990.

(2) Swift, D. L.; Friedlander, S. The coagulation of hydrosols by Brownian motion and laminar shear flow. *J. Colloid Sci.* **1964**, *19*, 621−647.

(3) Hidy, G. M. On the theory of the coagulation of noninteracting particles in Brownian motion. *J. Colloid Sci.* **1965**, *20*, 123−144.

(4) Smoluchowski, M. V. Solution of bivariate population balance equations using the finite size domain complete set of trial functions method of moments. *Z. Phys. Chem.* **1917**, *92*, 129−168.

(5) Drake, R. A general mathematical survey of the coagulation equation. *Top. Curr. Aerosol Res. (Part 2)* **1972**, *3*, 201−376.

(6) Muralidhar, R.; Ramkrishna, D. Analysis of droplet coalescence in turbulent liquid-liquid dispersions. *Ind. Eng. Chem. Fundam.* **1986**, *25*, 554−560.

(7) Ennis, B. J.; Tardos, G.; Pfeffer, R. A microlevel-based characterization of granulation phenomena. *Powder Technol.* **1991**, *65*, 257−272.

(8) Hounslow, M.; Mumtaz, H.; Collier, A.; Barrick, J.; Bramley, A. A micro-mechanical model for the rate of aggregation during precipitation from solution. *Chem. Eng. Sci.* **2001**, *56*, 2543−2552.

(9) Liew, T.; Barrick, J.; Hounslow, M. A Micro-mechanical model for the rate of aggregation during precipitation from solution. *Chem. Eng. Technol.* **2003**, *26*, 282−285.

(10) Patience, D.; Rawlings, J. Particle-shape monitoring and control in crystallization processes. *AIChE J.* **2001**, *47*, 2125−2130.

(11) Ramkrishna, D. *Population Balances: Theory and Applications to Particulate Systems in Engineering*; Academic Press: 2000.

(12) Wright, H.; Ramkrishna, D. Solutions of inverse problems in population balances I. Aggregation kinetics. *Comput. Chem. Eng.* **1992**, *16*, 1019−1038.

(13) Narsimhan, G.; Ramkrishna, D.; Gupta, J. P. Analysis of drop size distributions in lean liquid−liquid dispersions. *AIChE J.* **1980**, *26*, 991−1000.

(14) Narsimhan, G.; Nejfelt, G.; Ramkrishna, D. Breakage functions for droplets in agitated liquid−liquid dispersions. *AIChE J.* **1984**, *30*, 457−467.

(15) Sathyagal, A.; Ramkrishna, D.; Narsimhan, G. Solution of inverse problems in population balances-II. Particle break-up. *Comput. Chem. Eng.* **1995**, *19*, 437−451.

(16) Sathyagal, A.; Ramkrishna, D.; Narsimhan, G. Droplet breakage in stirred dispersions. Breakage functions from experimental drop-size distributions. *Chem. Eng. Sci.* **1996**, *51*, 1377−1391.

(17) Thompson, P. A transformation of the stochastic equation for droplet coalescence. Proceedings of the International Conference on Cloud Physics. 1968; pp 1115−1126.

(18) Bramley, A.; Hounslow, M.; Ryall, R. Aggregation during precipitation from solution: A method for extracting rates from experimental data. *J. Colloid Interface Sci.* **1996**, *183*, 155−165.

(19) Bramley, A.; Hounslow, M.; Ryall, R. Aggregation during precipitation from solution. Kinetics for calcium oxalate monohydrate. *Chem. Eng. Sci.* **1997**, *52*, 747−757.

(20) Raikar, N. B.; Bhatia, S. R.; Malone, M. F.; Henson, M. A. Self-similar inverse population balance modeling for turbulently prepared batch emulsions: Sensitivity to measurement errors. *Chem. Eng. Sci.* **2006**, *61*, 7421−7435.

(21) Patruno, L.; Dorao, C.; Dupuy, P.; Svendsen, H.; Jakobsen, H. Identification of droplet breakage kernel for population balance modelling. *Chem. Eng. Sci.* **2009**, *64*, 638−645.

(22) Patruno, L.; Dorao, C.; Svendsen, H.; Jakobsen, H. Analysis of breakage kernels for population balance modelling. *Chem. Eng. Sci.* **2009**, *64*, 501−508.

(23) Groh, A.; Krebs, J. Improved solution methods for an inverse problem related to a population balance model in chemical engineering. *Inverse Probl.* **2012**, *28*, 085006.

(24) Kostoglou, M.; Karabelas, A. On the self-similar solution of fragmentation equation: Numerical evaluation with implications for the inverse problem. *J. Colloid Interface Sci.* **2005**, *284*, 571−581.

(25) Kostoglou, M.; Karabelas, A. Toward a unified framework for the derivation of breakage functions based on the statistical theory of turbulence. *Chem. Eng. Sci.* **2005**, *60*, 6584−6595.

(26) Maaß, S.; Kraume, M. Determination of breakage rates using single drop experiments. *Chem. Eng. Sci.* **2012**, *70*, 146−164.

(27) Subramanian, G.; Ramkrishna, D. On the solutions of statistical models of cell populations. *Math. Biosci.* **1971**, *10*, 1−23.

DOI: 10.1021/acs.iecr.5b01368
Ind. Eng. Chem. Res. 2015, 54, 10530−10538

(28) Press, W. H.; Flannery, B. P.; Teukolsky, S. A.; Vetterling, W. T. *Numerical Recipes*; Cambridge University Press: Cambridge, 1990.
(29) Scott, W. T. Analytic studies of cloud droplet coalescence. *J. Atmos. Sci.* **1968**, *25*, 54−65.

DOI: 10.1021/acs.iecr.5b01368
Ind. Eng. Chem. Res. 2015, 54, 10530−10538